Thermodynamic Analysis of Light Olefins Production via Cracking of n-Hexane Using Gibbs Energy Minimization Approach and Analysis of Overall Reactions

Reza Khoshbin[1], Ramin Karimzadeh[1,*]

1. Chemical Engineering Department, Tarbiat Modares University, Jalal Al AhmadHighway,P.O.Box 4155-4838, Tehran, Iran.

ARTICLE INFO

Article history:
Received: September 11, 2017
Accepted: December 28, 2017

Keywords:
Thermodynamic analysis
Cracking
Light olefins

* Corresponding author: Ramin Karimzadeh
E-mail: Ramin@modares.ac.ir
Tel.: +98 21 82883315
Fax: +98 21 88006544

ABSTRACT

In this study,thermodynamic analysis of hexane cracking was conducted by Gibbs free energy minimization method and second law analysis of overall reactions. By-products were divided into three groups of methane, alkynes and aromatics and their possible production paths were discussed. Effect of operating conditions such as temperature and steam-to-hexane ratio on the cracking performance was also investigated. The principal set of compounds considered in the modelling was hydrogen, water, ethane, ethylene, acetylene, propane, propylene, methyl acetylene, butane, butylene and hexane. Results showed that Hexane conversion increased with increase of temperature and steam content. As temperature increased, the equilibrium olefin yield showed a volcano-shaped trend. In the presence of methane, the maximum olefin yield declined and shifted to lower temperatures. When aromatics were considered in the product list, the light olefins yield was negligible. Equilibrium predicted that adding steam to the feed stream led to the decrease of coke deposition through suppressing of aromatization reaction.

1. Introduction

In cracking process, hydrocarbons are heated to high temperatures. It leads to break the carbon-carbon bonds to give smaller fragments. This reaction is at the heart of all commercial technologies for upgrading hydrocarbons. Cracking of ethane and light liquid hydrocarbons including hexane and light naphtha is the conventional technique for the production of light olefins [1-4]. Light olefins such as ethylene and propylene are important starting material in petrochemical industries to produce polymers and various other petrochemicals [5, 6].

The cracking of n-alkanes, including n-hexane, heptanes and octane are often examined as a model feed for the naphtha catalytic cracking test to clarify catalysts performance [7, 8]. Most works presented in the literature have focused on the development of active and selective catalysts and the optimization of operating conditions for hexane cracking process [9-12]. However, the basic parameters including feed composition and temperature differ significantly among those researches and the results are hardly comparable. Moreover, durability of the cracking catalyst is one of the key factors in the development of catalytic cracking process. Coke deposition over catalyst is known as the main reason for the deactivation [13, 14]. Operating the cracking process at appropriate condition can inhibit such deactivation.

The thermodynamic analysis of hexane cracking provides the first step to analyze the limits of operating conditions on equilibrium products distribution and hexane conversions. Developing cracking reactors requires the thermodynamic and kinetic knowledge of liquid hydrocarbons reactions and product distributions. Despite the attention paid to the kinetic study of cracking, there has been few studies on the thermodynamic of liquid hydrocarbons cracking at severe operating conditions [15]. The ideal reaction pathway in hexane cracking is obtaining high olefin yield. However, undesirable side reactions including sequential dehydrogenation, aromatization and steam reforming may occur during the cracking of hexane. The reaction network depends on the operating conditions. Hence, thermodynamic studies are necessary to understand the relationships between operating conditions and the possible product distributions. The thermodynamic analysis makes it possible to evaluate if a determined operating condition for a specific reaction is technically viable or not, and to predict better operating conditions [16].

Chemical equilibrium calculations have been usually done using equilibrium constants of known reactions. This technique is useful for simple problems. Yan et al. [17] investigated thermodynamic properties of methane autothermal reforming reaction with this method. Nevertheless, when the composition of an equilibrium mixture is determined by a number of simultaneous reactions, calculations based on equilibrium constants get complicated. In these cases, using procedures which is based on the minimization of the total Gibbs energy is suitable [18, 19]. The beneficial use of Gibbs free energy minimization method is that a limited set of equations needs to be solved. In fact, each component present in the system can be treated independently without indicating sets of complicated reactions. Furthermore, the method requires only knowledge of Gibbs free energies of the components in a specified temperature and pressure.

In recent years, thermodynamic analysis of various processes including methanol steam reforming, dimethyl ether steam reforming, gasification process and methane steam reforming have been done [20-24]. Zhang et al. [25] investigated thermodynamically the effect of temperature and hydrocarbon pressure on olefin products distribution using Gibbs free energy minimization. However, effects of the steam-to-hydrocarbon ratio on products distribution were not discussed. Moreover, hexane cracking process is a complicated reaction which includes many side reactions. To the best of our knowledge, a detailed theoretical analysis of olefin production overall reactions through hexane cracking process has not been published yet.

Gibbs free energy is a suitable index to determine the reaction spontaneity. In this paper, a set of reactions for hexane cracking was considered and the effect of temperature on their Gibbs free energy was determined. Then, thermodynamic equilibrium composition of hexane cracking process was investigated. The influence of process variables such as temperature and steam-to-hexane ratio on hexane conversion and product distribution was also investigated to find out the optimal operating conditions for the cracking of hexane process. In this paper, results are reported as hexane conversion, olefin yield, aromatics and H_2 selectivity.

2. Modeling and Methodology

1.2. Thermodynamically Feasible Products

There are many reactions which take place during hexane cracking. Overall reactions for the formation of light olefins and by-products in hexane cracking process are listed in **Error! Reference source not found.**. The product set was expanded to consist of intermediate products or products from side reactions. As can be observed in this table, the proposed reactions were divided into five groups including formation reactions of light olefins, methane, aromatics, alkynes and C_2-C_4 alkanes.

Thermodynamically feasible reactions in the operating conditions range were predicted by the calculation of Gibbs free energy as a function of temperature. It was calculated using the 15-coefficients NASA polynomial as follows:

$$\frac{C_P^\circ}{R} = a_1 + a_2 T + a_3 T^2 + a_4 T^3 + a_5 T^4 \quad (1)$$

$$\frac{H_T^\circ}{RT} = \frac{\int C_P^\circ dT}{RT} = a_1 + \frac{a_2 T}{2} + \frac{a_3 T^2}{3} + \frac{a_4 T^3}{4} + \frac{a_5 T^4}{5} + \frac{a_6}{T} \quad (2)$$

$$\frac{S_T^\circ}{R} = \int \frac{C_P^\circ}{RT} dT = a_1 \ln T + a_2 T + \frac{a_3 T^2}{2} + \frac{a_4 T^3}{3} + \frac{a_5 T^4}{4} + a_7 \quad (3)$$

$$\frac{G_T^\circ}{RT} = \frac{H_T^\circ}{RT} - \frac{S_T^\circ}{R} = a_1(1 - \ln T) + \frac{a_2 T}{2} - \frac{a_3 T^2}{6} - \frac{a_4 T^3}{12} - \frac{a_5 T^4}{20} + \frac{a_6}{T} - a_7 \quad (4)$$

Where a_1-a_7 are the numerical coefficients supplied by Burcat.[26] Furthermore, C_p°, H_T°, S_T° and G_T° represent specific heat capacity, standard enthalpy, entropy and Gibbs free energy, respectively.

Table 1. Overall reactions of n-hexane cracking

No.	Reaction	No.	Reaction
Group A: light olefins formation reactions		R24	$C_3H_6 \leftrightarrow C_2H_2+CH_4$
R1	$C_6H_{14} \leftrightarrow 3C_2H_4+H_2$	R25	$C_6H_{14}+2CH_4 \leftrightarrow C_8H_{10}+6H_2$
R2	$C_6H_{14} \leftrightarrow 2C_3H_6+H_2$	Group C: aromatics formation reactions	
R3	$C_2H_6 \leftrightarrow C_2H_4+H_2$	R26	$C_6H_{14}+CH_4 \leftrightarrow C_7H_8+6H_2$
R4	$C_2H_4+C_2H_6 \leftrightarrow C_3H_6+CH_4$	R27	$C_6H_{14} \leftrightarrow C_6H_6+4H_2$
R5	$C_3H_8 \leftrightarrow C_3H_6+H_2$	R28	$C_2H_4+C_4H_6 \leftrightarrow C_6H_6+2H_2$
R6	$C_3H_8 \leftrightarrow C_2H_4+CH_4$	R29	$C_4H_6+C_3H_6 \leftrightarrow C_7H_8+2H_2$
R7	$2C_3H_6 \leftrightarrow 3C_2H_4$	R30	$C_4H_6+C_4H_6 \leftrightarrow C_8H_8+2H_2$
R8	$C_4H_{10} \leftrightarrow C_3H_6+CH_4$	R31	$2C_4H_6 \leftrightarrow C_8H_{10}+H_2$
R9	$C_4H_{10} \leftrightarrow C_2H_4+C_2H_6$	R32	$2C_3H_4 \leftrightarrow C_6H_6+H_2$
R10	$C_2H_2+H_2 \leftrightarrow C_2H_4$	Group D: alkyne formation reactions	
R11	$C_2H_2+CH_4 \leftrightarrow C_3H_6$	R33	$C_6H_{14} \leftrightarrow 3C_2H_2+4H_2$
R12	$C_6H_{14} \leftrightarrow C_3H_8+C_3H_6$	R34	$C_6H_{14} \leftrightarrow 2C_3H_4+3H_2$
R13	$C_6H_{14} \leftrightarrow C_2H_6+2C_2H_4$	R35	$C_6H_{14} \leftrightarrow n\text{-}C_4H_8+C_2H_2+2H_2$
R14	$C_6H_{14} \leftrightarrow n\text{-}C_4H_8+C_2H_4+H_2$	R36	$C_3H_6 \leftrightarrow C_3H_4+H_2$
R15	$C_6H_{14} \leftrightarrow C_2H_4+n\text{-}C_4H_{10}$	R37	$C_2H_4 \leftrightarrow C_2H_2+H_2$
R16	$C_3H_8+C_2H_4 \leftrightarrow C_2H_6+C_3H_6$	R38	$C_4H_8 \leftrightarrow C_4H_6+H_2$
R17	$C_4H_{10} \leftrightarrow 2C_2H_4+H_2$	R39	$C_2H_4+C_2H_2 \leftrightarrow C_4H_6$
R18	$C_6H_{14}+6H_2O \leftrightarrow 6CO+13H_2$	Group E: alkane formation reactions	
Group B: methane formation reactions		R40	$C_6H_{14} \leftrightarrow N\text{-}C_4H_8+C_2H_6$
R19	$C_4H_8 \leftrightarrow C_3H_4+CH_4$	R41	$C_6H_{14}+H_2 \leftrightarrow 3C_2H_6$
R20	$C_2H_4+2H_2 \leftrightarrow 2CH_4$	R42	$C_6H_{14} \leftrightarrow N\text{-}C_4H_8+C_2H_6$
R21	$C_3H_6+3H_2 \leftrightarrow 3CH_4$	R43	$C_6H_{14}+H_2 \leftrightarrow C_2H_6+N\text{-}C_4H_{10}$
R22	$2C_2H_6 \leftrightarrow C_3H_8+CH_4$	R44	$C_4H_{10} \leftrightarrow C_4H_8+H_2$
R23	$C_3H_6+C_2H_6 \leftrightarrow C_4H_8+CH_4$	R45	$C_4H_8 \leftrightarrow H_2+C_4H_6$

2.2. Gibbs Free Energy Minimization

For the sake of Gibbs Free Energy Minimization, the Lagrange multiplier method was used. Gibbs energy of the system can be written as follows:

$$G = RT.\sum_{k=1}^{m} n_k[(\frac{\mu^{\circ}}{RT}) + \ln \frac{\hat{f}_i}{f_i^0}] \quad (5)$$

The material balance for a system comprised of w elements can be expressed as Equation (6):

$$\sum_{k=1}^{m} a_{kj}.n_k = b_j \quad (6)$$

Where k is a particular atom and a_{kj} is the number of atoms of the k^{th} element in a molecule of the j^{th} substance in the system. Moreover, b_j represents the amount of jth element in the system. Gibbs energy minimization was done by the Lagrange multiplier method. With this method, the minimum of

Gibbs energy is subjected to the mass balance relations. The new objective function to be minimized in terms of the amounts of matter n_k is written as:[27]

$$L = F - \lambda_j (\sum_{k=1}^{m} a_{kj} n_k - b_j) \quad (7)$$

Where λ_i are the Lagrange undefined multipliers. The minimum of L gives the minimum of F while the mass balance condition Equation (6) holds. The respective partial derivatives in terms of the amounts (n_k) must be zero. Therefore, the equation to be solved is as follows:

$$[\frac{\partial F}{\partial n_j}]_{T,P,n_k} - \sum_{j=1}^{NC} \lambda_j . a_{kj} = 0 \qquad \text{(k=1,2, ..., m)} \quad (8)$$

The first term on the left is the definition of the chemical potential;

$$\mu_k + \sum_j \lambda j a_{kj} = 0 \qquad \text{(k=1,2, ..., m)} \quad (9)$$

Therefore, for gas-phase reactions at Pº, this equation can be written as follows:

$$\mu_k = \Delta G^{\circ}_{f_k} + RT \ln \frac{y_k \hat{\varphi}_k P}{P^{\circ}} \qquad \text{(k=1,2, ..., N)} \quad (10)$$

Combination with Equation (9) gives:

$$\Delta G^{\circ}_{f_k} + RT \ln \frac{y_k \hat{\varphi}_k P}{P^{\circ}} + \sum_j \lambda_j a_{kj} = 0 \qquad \text{(k=1,2, ..., N)} \quad (11)$$

where ΔGº is the standard Gibbs function of formation of species i, R is the molar gas constant, T is the processing temperature, P is the processing pressure, yi is the gas phase mole fraction of species i and $\hat{\varphi}_i$ is the fugacity coefficient of species i. There are N equilibrium equations in Equation (11), one for each chemical species. Moreover, there are w Material balances in Equation (6). Therefore, the number of total equations is N +w.

This method is based on minimizing the total Gibbs free energy in the system without the specification of the plausible reactions taking place. However, this requires the identification of the plausible products. In this paper, possible products were classified into three cases as follows:

- Case 1: Hydrogen, water, ethane, ethylene, acetylene, propane, propylene, methyl acetylene, butane, butylene and hexane
- Case 2: Hydrogen, water, methane, ethane, ethylene, acetylene, propane, propylene, methyl acetylene, butane, butylene and hexane
- Case 3: Hydrogen, water, methane, ethane, ethylene, acetylene, propane, propylene, methyl acetylene, butane, butylene, hexane, benzene, xylene and toluene

As can be seen above, methane was added to product set in the second case. In the third case, in addition to methane, aromatics such as benzene, xylene and toluene were considered in the predicted products. The modelling

methodology was conducted through a sequential procedure. At first, the reactants and their relative proportions were chosen. Then, products were chosen. In the third step, operating conditions such as temperature and steam-to-hexane ratio were chosen and minimization was performed. Next, the calculated results were consecutively analyzed for an optimal condition of the cracking process.

The steam-to-hexane weight ratio and reaction temperature were varied in the range of 0–1 and 500-1300K, respectively. It should be noted that the Peng–Robinson equation was used as the equation of state.

Hexane conversion, light olefins yield, propylene, ethylene, aromatics and hydrogen selectivity were calculated as follows:

$$X_{HEX}\,(wt\%) = \left(\frac{F_{HEX_{in}} - F_{HEX_{out}}}{F_{HEX_{in}}}\right) \times 100 \quad (12)$$

$$Yield_{\,E,P}(wt\%) = \left(\frac{F_{E,P}}{F_{HEX_{in}}}\right) \times 100 \quad (13)$$

$$S_{ethylene}(wt\%) = \left(\frac{F_{ethylene}}{F_{products}}\right) \times 100 \quad (14)$$

$$S_{propylene}(wt\%) = \left(\frac{F_{propylene}}{F_{products}}\right) \times 100 \quad (15)$$

$$S_{aromatics}(wt\%) = \left(\frac{F_{aromatics}}{F_{products}}\right) \times 100 \quad (16)$$

$$S_{H_2}(wt\%) = \left(\frac{F_{H_2}}{F_{products}}\right) \times 100 \quad (17)$$

Where ‘‘$F_{HEX_{in}}$”,“$F_{HEX_{out}}$”, “$F_{E,P}$”, “$F_{ethylene}$”, “$F_{propylene}$” “$F_{aromatics}$”, “F_{H_2}” are the mass flow rates of hexane in feed and product streams, olefins, ethylene, propylene, aromatics and hydrogen, respectively.

3. Results and Discussion

3.1. Effect of Temperature on Gibbs free energy of Hexane Cracking Reactions

Gibbs free energy of hexane pyrolysis reactions was calculated. As Figure 1 shows the direct conversion of hexane to ethane and ethylene (R13) begins at temperature higher than 340K. Furthermore, ethylene and propylene formation through hexane dehydrogenation reactions (R1, R2) do not become favourable until temperature reaches beyond 800K. On the other hand, the hexane dehydrogenation reaction for the production of butylene and ethylene (R14) is not favourable in the studied temperature range. Furthermore, it can be observed that acetylene and methyl acetylene formation reactions (R33, R34) are favourable at temperatures higher than 1100K. It should be noted that Gibbs free energy of other reactions declined with increasing of reaction temperature.

The effect of temperature on Gibbs free energy of light olefins formation reactions are shown in Figure 2. At first glance, it can be observed that reactions (R4) and (R16) are independent of temperature. They can be done all over the reaction temperature range. However, their magnitude of ΔG is relatively low, meaning that the presence of either the product or reactant species could drive the reaction in either direction. Furthermore, it can be seen that increasing temperature has got a retarding effect on the proceeding acetylene hydrogenation reaction (R10) and combination reaction of methane and acetylene (R11). Gibbs energy of the other listed reactions shows a descending trend. It means that by increasing the reaction temperature, their spontaneity gradually increases.

Formation of many by-products is one of the main drawbacks of cracking liquid hydrocarbons process. These by-products can be divided into three groups of methane, alkynes and aromatics. In this section, their possible production paths are discussed.

Methane is one of the important by-products in the cracking of hexane. The effect of temperature on Gibbs free energy of methane production reactions is depicted in Figure 3. As can be seen in this figure, whole of reactions take place above 775 K spontaneity. The decomposition of butylene to methyl acetylene and methane (R19) is spontaneity above 750K. Because of lower Gibbs energy of ethylene and propylene hydrogenation reactions (R20, R21), the possibility of methane formation via these reactions is higher than the other reactions. Furthermore, results showed that as temperature increased, Gibbs free energy of propane and butane pyrolysis (R6, R8) got lower. Therefore, increasing temperature led to increasing methane formation through these paths. In addition, results indicated that other reactions are invariant under changes in the temperature.

Figure 4 provides details about Gibbs free energy of alkynes formation reactions. As can be seen in this figure, methyl acetylene can be produced through butylene pyrolysis (R19) at greater than 775K. In addition, propylene pyrolysis (R24) can be done spontaneously at temperature higher than 975K. The high temperature was benefited to conduct the direct conversion of hexane to alkynes reactions (R33, R34). It can be observed that they begin at higher than 1100K. Furthermore, dehydrogenation of ethylene and butylene for the production of acetylene and butyne (R37, R38) need to consume much energy. They can proceed at temperatures above 1300K and 1400K, respectively. On the other hand, butyne can be formed through the combination of ethylene and acetylene (R39) up to 970K. As reaction temperature exceeds 970K, this reaction suppresses.

Aromatics are the most undesirable by-products in the cracking of hexane. These components aggregate and deposit as coke on the reactor wall or catalyst surface. This phenomenon not only increases energy consumption, but also decreases product yield significantly [4]. The aromatization of hexane occurs in various paths. As mentioned above, hexane may transform to alkenes in two routes of cracking and dehydrogenation reactions. However, alkenes may convert to aromatics through oligomerization, cyclization and dehydrogenation reactions [28]. Furthermore, reactions which occur between byproducts such as alkynes and methane cause the formation of aromatics.

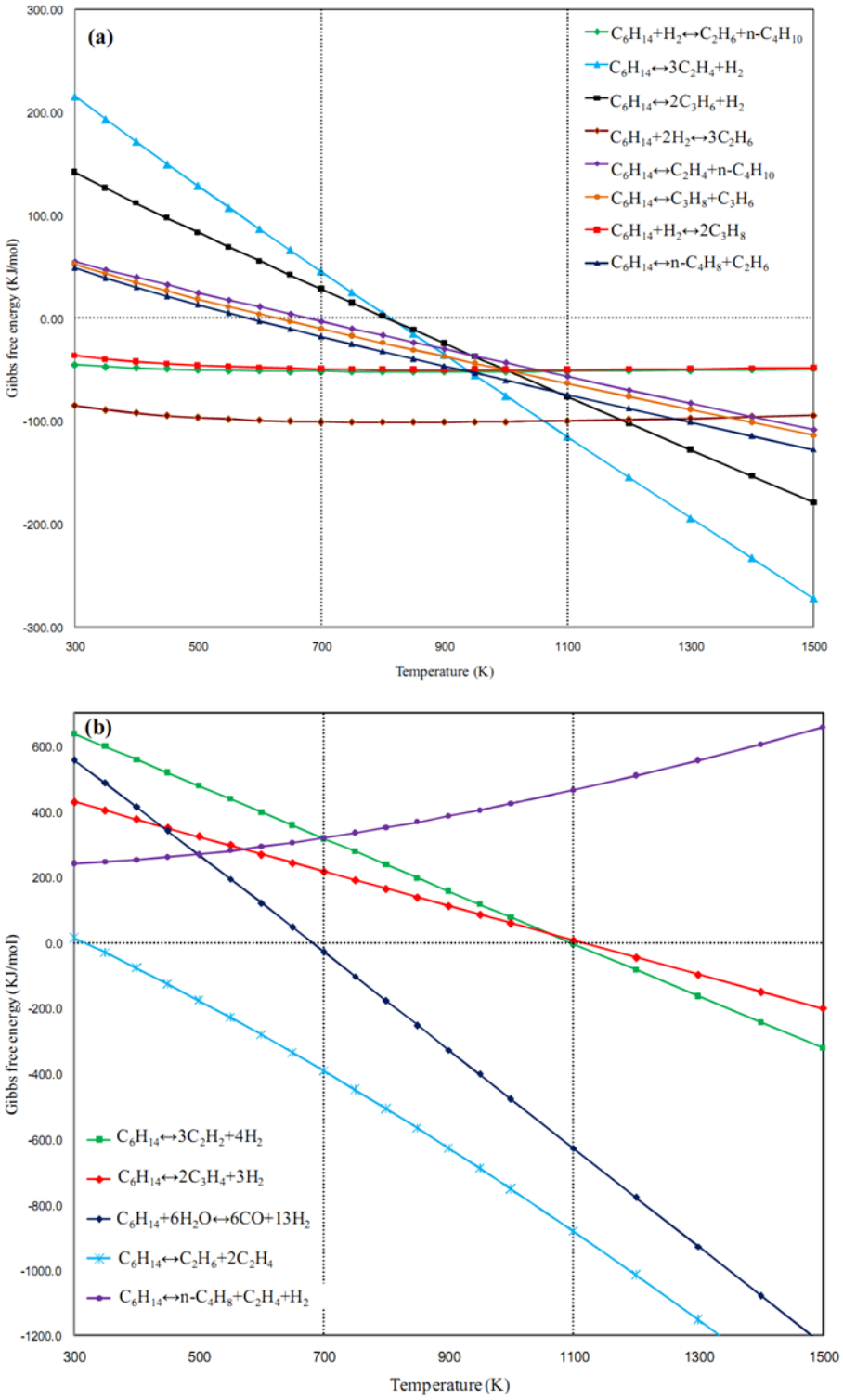

Figure 1. (a) and (b) Gibbs free energy of hexane pyrolysis reactions

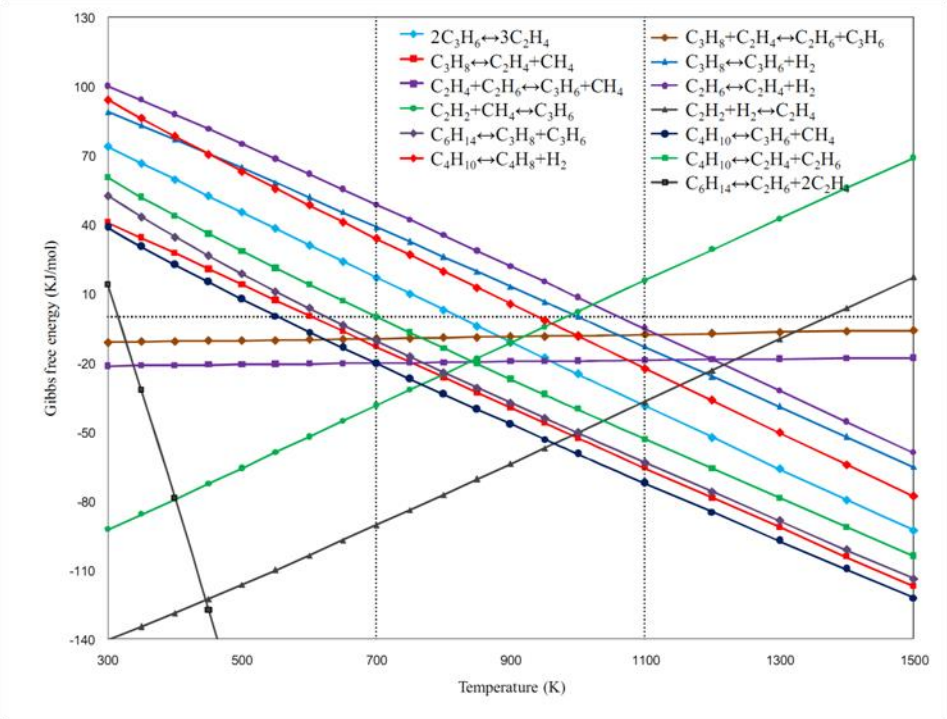

Figure 2. Gibbs free energy of light olefins formation reactions

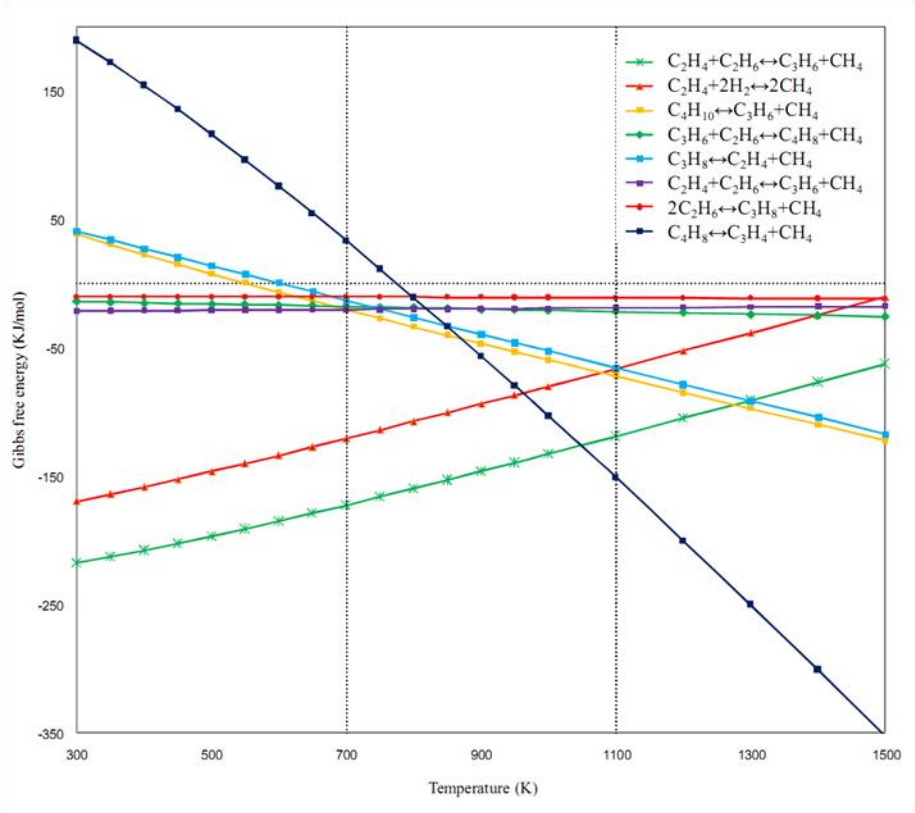

Figure 3. Gibbs free energy of methane formation reactions

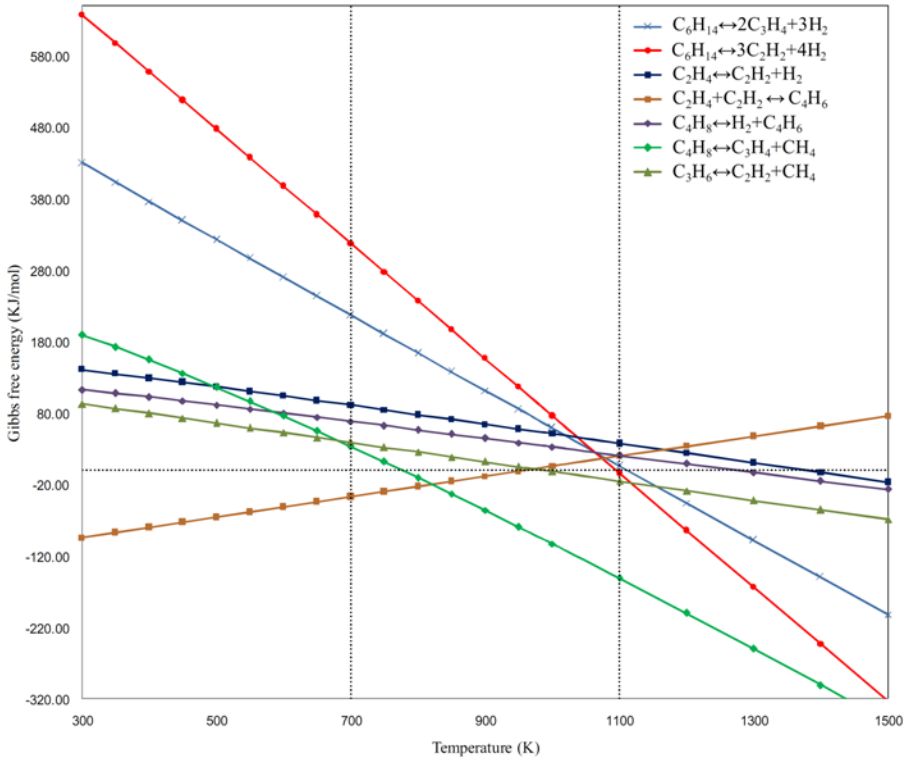

Figure 4.Gibbs free energy of alkynes formation reactions

Figure 5 depicts Gibbs free energy of aromatic reaction formation. According to this figure, most of assumed reaction can proceed spontaneously in the studied temperature range. Xylene, toluene and benzene formation through reactions R25, R26 and R27 become spontaneity at 450, 550 and 600K, respectively. The increasing reaction temperature facilitates the aromatization reactions.

3.2. Effect of Temperature and Steam Content on Hexane Conversion

The equilibrium conversion of hexane as a function of reaction temperature and steam-to-hexane ratio is shown in Figure 6. In the absence of aromatic compounds (Figure 6.a-b), hexane conversion depended on temperature and steam content. In the absence of methane (case 1), when temperature increased from 500 to 700K, hexane conversion increased from 82 to 100%. After that, hexane conversion remained 100% until 1300K. It can be attributed to endothermic nature of the hexane cracking reaction. When methane was added to product list (case 2), the minimum of hexane conversion increased from 82 to 91%. In addition, increase of steam content in the feed stream led to increase the hexane conversion. For instance in case 1, at constant temperature of 500K, as steam-to-hexane ratio increased from 0 to 0.4, hexane conversion increased from 82 to 100%. However, in temperature range higher than 600K, hexane conversion was independent of steam content.

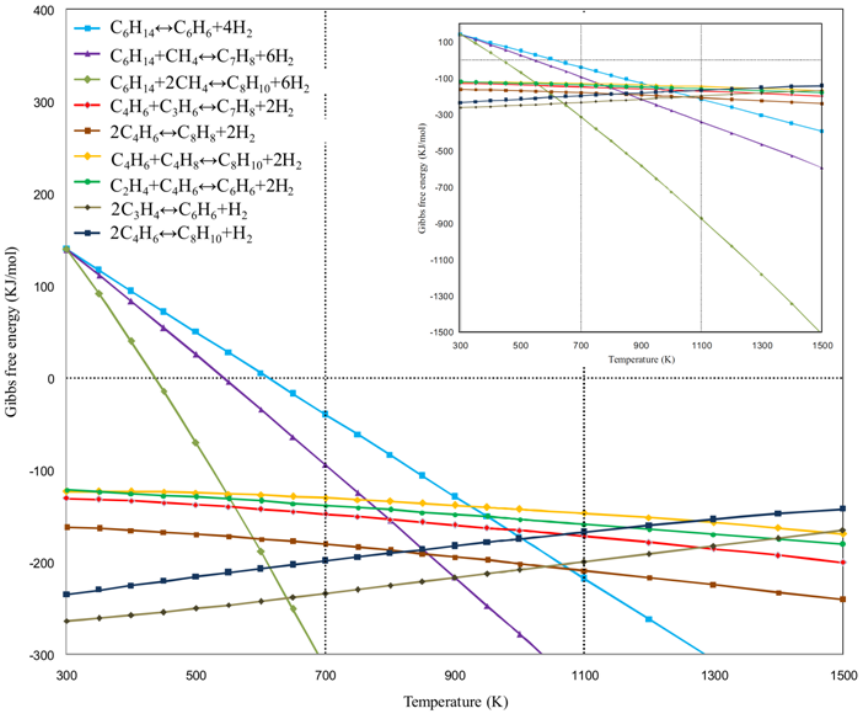

Figure 5. Gibbs free energy of aromatics formation reactions

Increased conversion of hexane along with increase in temperature was experimentally observed by Mochizuki et al.[29] during the catalytic cracking of n-hexane.

On the other hand, when aromatics were considered in the product list, the conversion of hexane was not limited by equilibrium. It can be observed that the complete conversion of hexane is achieved throughout the operating condition range. According to Figure 5, Gibbs free energy of hexane to aromatics reactions are negative even at low temperatures. Therefore, when aromatics are considered in product set, hexane conversion reaches 100% due to the aromatization of hexane reactions.

3.3. Effect of Temperature and Steam Content on the Olefin Yield

Effect of operating conditions on the equilibrium olefins yield has been shown in Figure 7. Temperature has a significant effect on the olefin yield. According to Figure 7.a (case 1), as temperature increases, the equilibrium olefin yield shows a volcano trend. The highest equilibrium olefins yield is 81% which can be obtained at 1100K. However, in the presence of methane (case 2) the temperature, in which the maximum olefin produced, shifted to lower temperature (800K). Moreover, the highest obtained olefin yield decreased to 64%. The descending trend of olefins yield at higher temperatures can be attributed to the decrease of propylene yield.

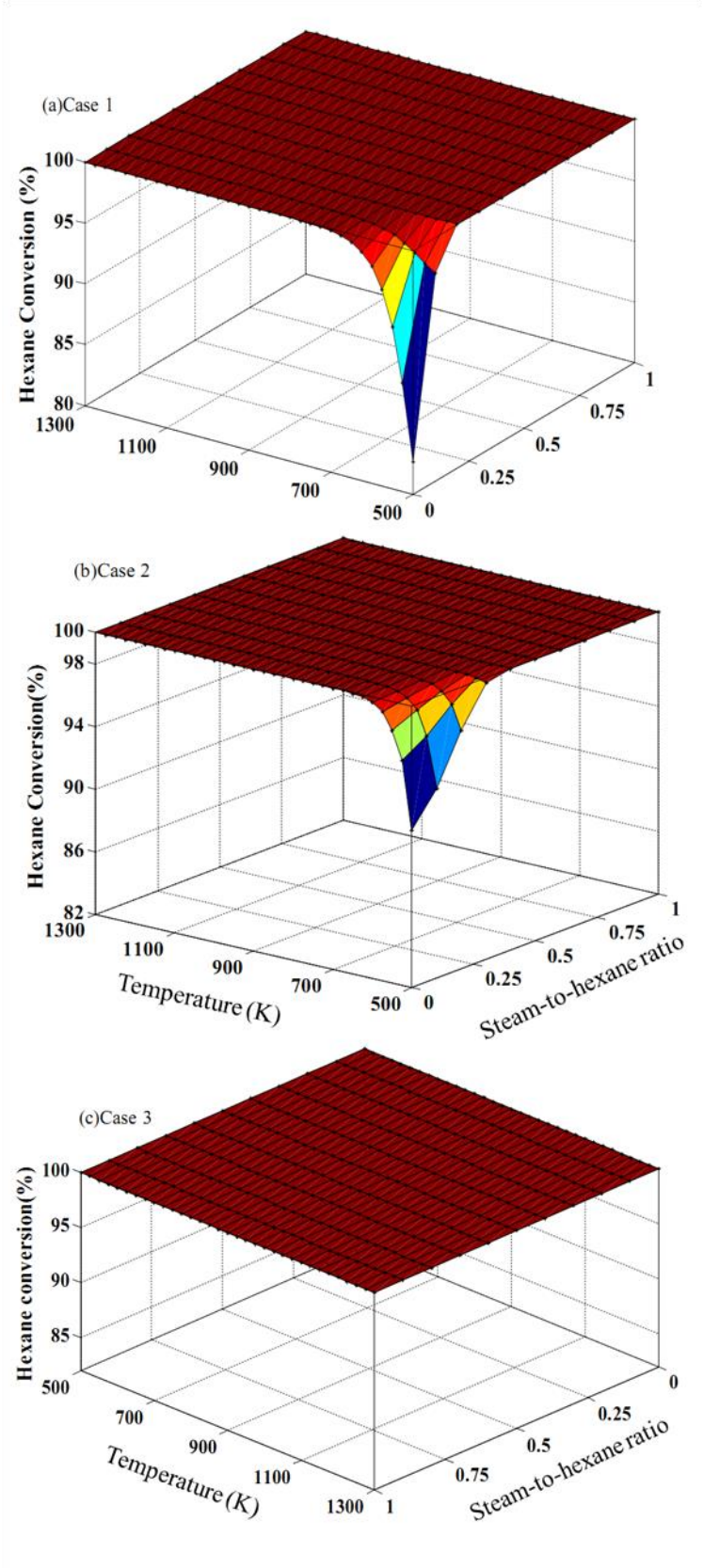

Figure 6. Effect of temperature and steam to hexane ratio on the equilibrium conversion of hexane

The effect of temperature on propylene and ethylene selectivity in the absence of steam are calculated and shown in Figure 8. Results show that in case 1 and 2, propylene yield increases by increasing temperature and goes through a maximum value at 750K and 775K, respectively and then decreases at higher temperatures. However, the ethylene yield increases with enhancement of reaction temperature and falls at above 1025K and 1150K in case 1 and 2, respectively. The decline of propylene yield may be attributed to the conversion of propylene to ethylene reaction through reaction (R7).The more decline of propylene yield in case 2 may be attributed to the conversion of propylene to acetylene reaction (R24). Mochizuki et al.[30] studying hexane cracking over ZSM-5 catalysts, observed a similar behaviour during their experiments. As can be seen in Figure 4, Gibbs free energy of propylene conversion to acetylene reaction (R24) shows a descending trend and at 970K, it reaches zero. Therefore, at temperatures higher than 900K this reaction can take place spontaneously. Results from equilibrium calculation show that as temperature increases from 900K to 1300K, the acetylene selectivity also increases from 2.5% to 38%. Enhancement of steam content in the feed stream led to decline the olefins yield. As mentioned in Figure 1, Gibbs free energy of hexane reforming reaction is less than the other hydrogenation reaction. When the steam content increased, the reforming reaction competed with cracking reaction to consume hexane. Therefore, the olefin yield decreased significantly.

On the other hand, in case 3 the olefins yield decreased remarkably. It can be seen that the highest obtained olefins yield is about 1.3%. The equilibrium selectivity of aromatics in case 3 is shown in Figure 9. At first glance, it can be observed that in lower steam content and higher temperature, the aromatics are the main products. For instance, in steam free feed stream condition, the obtained aromatics selectivity is more than 50%. As steam content increased, the aromatics selectivity decreased due to the expedition of hexane reforming reaction. It can be concluded that when aromatics are considered in the product set, most of hexane converted to the aromatics instead of olefins. In equilibrium analysis, the kinetic limits dose is not considered and the obtained results is ascribed to the high contact time conditions. Therefore, the low obtained olefin yield in case 3 can be ascribed to the complete transformation of ethylene and propylene into aromatics through sequential reactions in long contact time.

This result is in line with obtained results from Figure 5. According to this figure, most of the aromatization reactions are favourable thermodynamically. The larger negative values of their Gibbs free energy show further proceeding of aromatization reaction to the right-hand side. For this reason, a great effort take place to the development of catalysts that can minimize residence time of feed in the catalysts pores. Konno et al.[31] showed that reduction of crystallite size of the ZSM-5 catalysts inhibited the formation of coke on in the pore during the catalytic cracking of hexane. Furthermore, Tago et al.[32] showed that using catalysis with moderate catalyst acidity led to control the sequential reactions. Therefore, the aromatics selectivity decreased significantly.

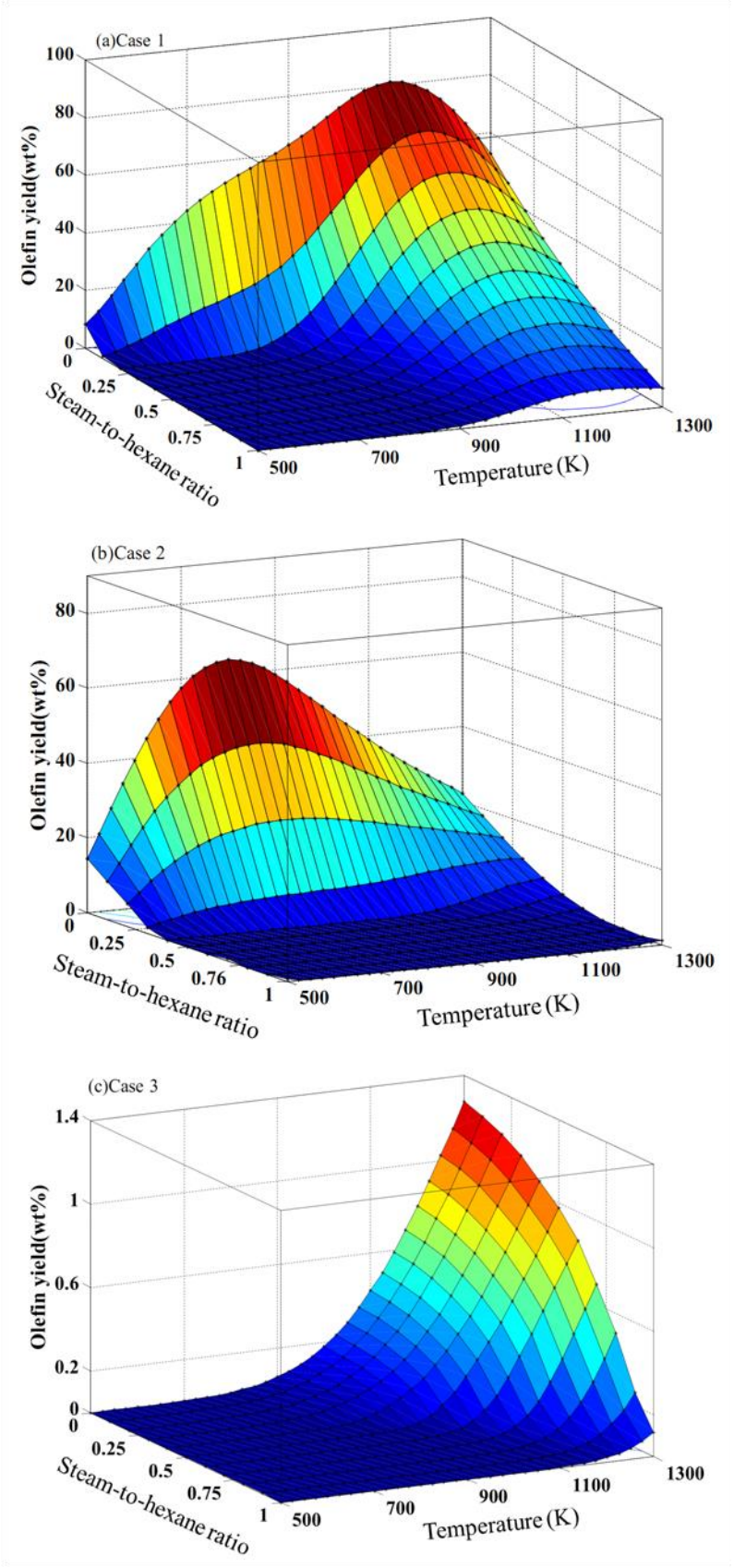

Figure 7. Effect of temperature and steam to hexane ratio on the equilibrium olefin yield

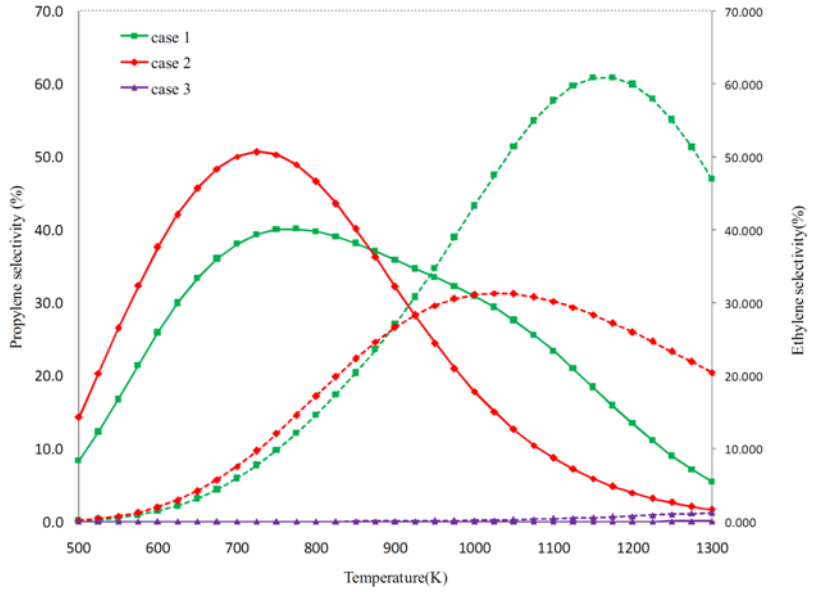

Figure 8. Effect of temperature on the equilibrium olefin selectivity in no steam condition

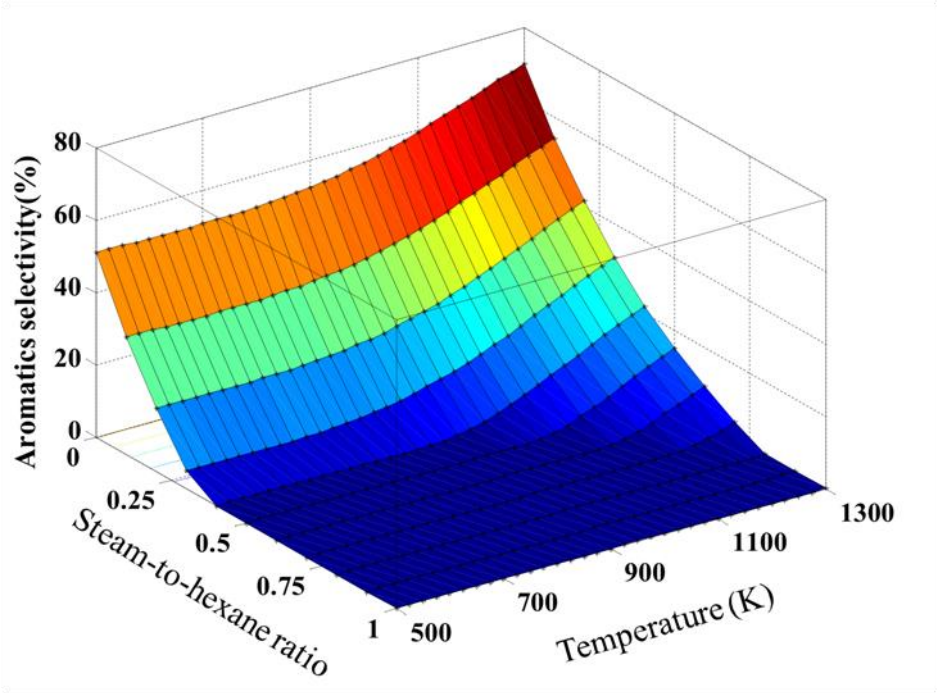

Figure 9. Effect of temperature and steam to hexane ratio on the equilibrium aromatics selectivity

3.4. Effect of Temperature and Steam Content on the Hydrogen Selectivity

Figure 10 illustrates equilibrium hydrogen selectivity as a function of operating conditions. Results show that there was a similar trend in hydrogen selectivity in all cases. In case 1 and 2, at low steam content conditions, hydrogen could be produced through alkanes dehydrogenation reactions (e.g. R1, R2, R3, R5, R17 and so on). However, the obtained hydrogen in case 3 could be attributed to aromatization reactions (R25-R32). The most of considered aromatization reactions in this study can be classified into the dehydrogenation reaction group.

According to this figure, when the steam content increased, the hydrogen selectivity increased remarkably. Increasing the steam-to-hexane ratio more than 0.4 introduced more steam than required for cracking; therefore, a transitioning from hexane cracking to hexane reforming occurred above steam-to-carbon ratio of 0.4. Furthermore, the increase of reaction temperature led to increase the amount of hydrogen production. It may be due to the endothermic nature of hexane cracking and reforming reactions. Similar trend has been reported in the literature by Al-Musa et al.[33] for steam reforming of liquid hydrocarbons.

4. Conclusion

A comprehensive thermodynamic analysis of hexane cracking overall reactions was carried out to investigate the light olefins production routs. By-products were divided into three groups of methane, alkynes and aromatics and their possible production paths were discussed. In addition, a thermodynamic chemical equilibrium of hexane cracking process was investigated using Gibbs free energy minimization method. The principal set of compounds considered in the modelling included hydrogen, water, ethane, ethylene, acetylene, propane, propylene, methyl acetylene, butane, butylene and hexane. When temperature increased from 500 to 700K, hexane conversion increased from 82 to 100%. After that, hexane conversion remained 100% until 1300K. Increase of steam content in the feed stream led to increase the hexane conversion. As temperature increased, the equilibrium olefin yield showed a volcano trend. The maximum olefin yield was obtained at steam free conditions. Enhancement of the steam content in the feed stream led to decline the olefins yield due to the competition between hexane cracking and reforming reaction in the hexane consumption. When aromatics were taken into account, the conversion of hexane was not limited by equilibrium. Furthermore, the increase of steam content in feed mixture caused the decrease of aromatics selectivity. When the steam content increased, the hydrogen selectivity increased remarkably.

Furthermore, the increase of reaction temperature led to increase the amount of hydrogen production. Equilibrium predicted that adding steam to the feed stream would lead to the decrease of coke deposition through suppressing of the aromatization reaction. Assuming that all kinetic restrictions could be overcome, results indicated that at high contact times, the steam-to-hexane ratios of 0.1-0.2 would be suitable to perform hexane cracking by considering a balance between the advantages and disadvantages.

It should be noted that in order to provide a full description of hexane cracking process, kinetic limitation should be studied as a future line of research.

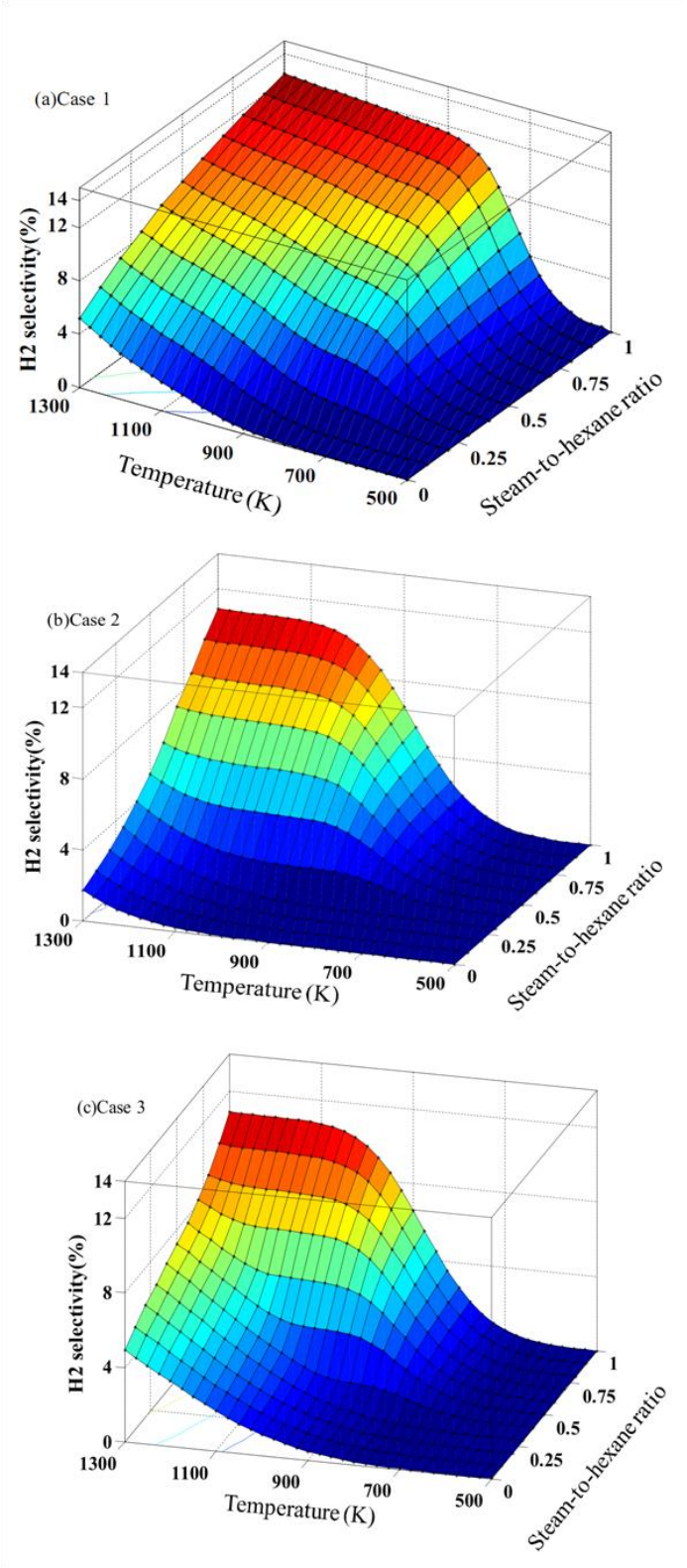

Figure 10. Effect of temperature and steam to hexane ratio on the equilibrium hydrogen selectivity

Nomenclature

$a_{k,j}$	number of atoms of the k^{th} element present in each molecule of species i
a_1,.., a_7	NASA polynomial coefficients
b_j	amount of j^{th} element in the system
C_P°	specific heat capacity
$F_{aromatics}$	mass flow rate of aromatics in product stream
$F_{ethylene}$	mass flow rate of ethylene in product stream
$F_{E,P}$	mass flow rate of light olefins in product stream
F_{H_2}	mass flow rate of hydrogen in product stream
$F_{HEX_{in}}$	mass flow rate of hexane in feed stream
$F_{HEX_{out}}$	mass flow rate of hexane in product stream
$F_{propylene}$	mass flow rate of propylene in product stream
$F_{products}$	mass flow rate of product stream
G_i°	standard Gibbs free energy of species i
$\Delta G_{f_i}^\circ$	standard Gibbs function of formation of species i
H_i°	standard enthalpy of species i
N	number of species in the reaction system
P°	standard-state pressure of 101.3 kPa
R	molar gas constant
$S_{aromatics}$	Aromatics selectivity
$S_{ethylene}$	ethylene selectivity
S_{H_2}	hydrogen selectivity
$S_{propylene}$	propylene selectivity
S_i°	standard entropy of species i
T	temperature of system (K)
y_i	gas phase mole fraction
$Yield_{P,E}$	Light olefins yield

Greek symbols

$\hat{\varphi}_i$	fugacity coefficient of species i
λ_k	Lagrange multiplier
μ_i	chemical potential of species i

References

[1] M., Berreni, M. Wang, "*Modelling and dynamic optimization of thermal cracking of propane for ethylene manufacturing".* Computers & Chemical Engineering, 2011. 35(12): p. 2876-2885.

[2] P. Ranjan, P. Kannan, A. Al Shoaibi, C. Srinivasakannan, "*Modeling of Ethane Thermal Cracking Kinetics in a Pyrocracker".* Chemical Engineering & Technology, 2012. 35(6): p. 1093-1097.

[3] S.M. Sadrameli, A.E.S. Green, "*Systematics and modeling representations of naphtha thermal cracking for olefin production".* Journal of Analytical and Applied Pyrolysis, 2005. 73(2): p. 305-313.

[4] T. Ren, M. Patel, K. Blok, "*Olefins from conventional and heavy feedstocks: Energy use in steam cracking and alternative processes".* Energy, 2006. 31(4): p. 425-451.

[5] A. Ramírez, J.L. Hueso, R. Mallada, J. Santamaría, "*Ethylene epoxidation in microwave heated structured reactors".* Catalysis Today, 2016. 273: p. 99-105.

[6] A. Prieto, M. Palomino, U. Díaz, A. Corma, "*One-pot two-step process for direct propylene oxide production catalyzed by bi-functional Pd(Au)@TS-1 materials".* Applied Catalysis A: General, 2016. 523: p. 73-84.

[7] Y. Kubota, S. Inagaki, K. Takechi, "*Hexane cracking catalyzed by MSE-type zeolite as a solid acid catalyst".* Catalysis Today, 2014. 226 :p. 109-116.

[8] Y. Wang, T. Yokoi, S. Namba, J.N. Kondo, T. Tatsumi, "*Catalytic cracking of n-hexane for producing propylene on MCM-22 zeolites".* Applied Catalysis A: General, 2015. 504: p. 192-202.

[9] Y. Wang, R. Otomo, T. Tatsumi, T. Yokoi, " *Dealumination of organic structure-directing agent (OSDA) free beta zeolite for enhancing its catalytic performance in n-hexane cracking".* Microporous and Mesoporous Materials, 2016. 220: p. 275-281.

[10] Y. Wang, T. Yokoi, S. Namba, J.N. Kondo, T. Tatsumi, "*Improvement of catalytic performance of MCM-22 in the cracking of n-hexane by controlling the acidic property".* Journal of Catalysis, 2016. 333: p. 17-28.

[11] A. Yamaguchi, D. Jin, T. Ikeda, K. Sato, N. Hiyoshi, T. Hanaoka, F. Mizukami, M. Shirai, "*Deactivation of ZSM-5 zeolite during catalytic steam cracking of n-hexane".* Fuel Processing Technology, 2014. 126: p. 343-349.

[12] A. Yamaguchi, D. Jin, T. Ikeda, K. Sato, N. Hiyoshi, T. Hanaoka, F. Mizukami, M. Shirai, "*Effect of steam during catalytic cracking of n-hexane using P-ZSM-5 catalyst".* Catalysis Communications, 2015. 69: p. 20-24.

[13] R. Javaid, K. Urata, S. Furukawa, T. Komatsu, "*Factors affecting coke formation on H-ZSM-5 in naphtha cracking".* Applied Catalysis A: General,2015. 491: p. 100-105.

[14] K. Urata, S. Furukawa, T. Komatsu, "*Location of coke on H-ZSM-5 zeolite formed in the cracking of n-hexane".* Applied Catalysis A: General, 2014. 475: p. 335-340.

[15] N. Jia, R.G. Moore, S.A. Mehta, M.G. Ursenbach, "*Kinetic modeling of thermal cracking reactions".* Fuel, 2009. 88(8): p. 1376-1382.

[16] C.C.R.S. Rossi, C.G. Alonso, O.A.C. Antunes, R. Guirardello, L. Cardozo-Filho, "*Thermodynamic analysis of steam reforming of ethanol and glycerine for hydrogen production".* International Journal of Hydrogen Energy, 2009. 34(1): p. 323-332.

[17] Y. Yan, J. Zhang, L. Zhang, "*Properties of thermodynamic equilibrium-based methane autothermal reforming to generate hydrogen".* International Journal of Hydrogen Energy, 2013. 38(35): p. 15744-15750.

[18] C.C.R.S. Rossi, L. Cardozo-Filho, R. Guirardello, "*Gibbs free energy minimization for the calculation of chemical and phase equilibrium using linear programming".* Fluid Phase Equilibria, 2009. 278(1-2): p. 117-128.

[19] Y. LWIN, "*Chemical Equilibrium by Gibbs Energy Minimization on Spreadsheets".* International Journal of Engineering Education, Int. J. Engng Ed. 16(4): p. 335-339.

[20] T.A. Semelsberger, R.L. Borup, "*Thermodynamic equilibrium calculations of hydrogen production from the combined processes of dimethyl ether steam reforming and partial oxidation".* Journal of Power Sources, 2006. 155(2): p. 340-352.

[21] K. Faungnawakij, R. Kikuchi, K. Eguchi, "*Thermodynamic analysis of carbon formation boundary and reforming performance for steam reforming of dimethyl ether".* Journal of Power Sources, 2007. 164(1): p. 73-79.

[22] T. Renganathan, M.V. Yadav, S. Pushpavanam, R.K. Voolapalli, Y.S. Cho, "*CO_2 utilization for gasification of carbonaceous feedstocks: A thermodynamic analysis".* Chemical Engineering Science, 2012. 83: p. 159-170.

[23] K. Faungnawakij, R. Kikuchi, K. Eguchi, "*Thermodynamic evaluation of methanol steam reforming for hydrogen production".* Journal of Power Sources, 2006. 161(1): p. 87-94.

[24] Y. Sun, T. Ritchie, S.S. Hla, S. McEvoy, W. Stein, J.H. Edwards, "*Thermodynamic analysis of mixed and dry reforming of methane for solar thermal applications".* Journal of Natural Gas Chemistry, 2011. 20(6): p. 568-576.

[25] R. Zhang, Z. Wang, H .Liu, Z. Liu, G. Liu, X. Meng, "T*hermodynamic equilibrium distribution of light olefins in catalytic pyrolysis".* Applied Catalysis A: General, 2016. 522: p. 165-171.

[26] A. Burcat, *Thermochemical Data for Combustion Calculations*, in *Combustion Chemistry*, W.C. Gardiner, Editor. 1984, Springer US: New York, NY. p. 455-473.

[27] D. Green, R. Perry, *Perry's Chemical Engineers' Handbook, Eighth Edition*. 2007, New York: McGraw-Hill Education.

[28] L.H. Nguyen, T. Vazhnova, S.T. Kolaczkowski, D.B. Lukyanov, "*Combined experimental and kinetic modelling studies of the pathways of propane and -butane aromatization over H-ZSM-5 catalyst".* Chemical Engineering Science, 2006. 61(17): p. 5881-5894.

[29] H. Mochizuki, T. Yokoi, H. Imai, S. Namba, J.N. Kond, T. Tatsumi, "*Effect of desilication of H-ZSM-5 by alkali treatment on catalytic performance in hexane cracking".* Applied Catalysis A: General, 2012. 449: p. 188-197.

[30] H. Mochizuki, T. Yokoi, H. Imai, R. Watanabe, S. Namba, J.N. Kondo, T. Tatsumi, "*Facile control of crystallite size of ZSM-5 catalyst for cracking of hexane".* Microporous and Mesoporous Materials, 2011. 145(1-3): p. 165-171.

[31] H. Konno, T. Okamura, T. Kawahara, Y. Nakasaka, T. Tago, T. Masuda, "*Kinetics of n-hexane cracking over ZSM-5 zeolites-Effect of crystal size on effectiveness factor and catalyst lifetime".* Chemical Engineering Journal, 2012. 207-208: p. 490-496.

[32] T. Tago, H. Konno, Y. Nakasaka, T. Masuda, "*Size-Controlled Synthesis of Nano-Zeolites and Their Application to Light Olefin Synthesis".* Catalysis Surveys from Asia, 2012. 16(3): p. 148-163.

[33] A. Al-Musa, M. Al-Saleh, Z.C. Ioakeimidis, M. Ouzounidou, I.V. Yentekakis, M. Konsolakis, G.E. Marnellos, "*Hydrogen production by iso-octane steam reforming over Cu catalysts supported on rare earth oxides (REOs)".* International Journal of Hydrogen Energy, 2014. 39(3): p. 1350-1363.

آنالیز ترمودینامیکی تولید اولفین‌های سبک از طریق کراکینگ هگزان به روش حداقل سازی انرژی گیبس و آنالیز واکنش‌های کلی به کمک قانون دوم ترمودینامیک

رضا خوش‌بین [1]، رامین کریم‌زاده [1،*]

1. تهران، دانشگاه تربیت مدرس، دانشکده مهندسی شیمی، صندوق پستی ۴۸۳۸-۴۱۵۵

مشخصات مقاله

تاریخچهٔ مقاله:
دریافت: ۲۰ شهریور ۱۳۹۶
پذیرش نهایی: ۷ دی ۱۳۹۶

کلمات کلیدی:
آنالیز ترمودینامیکی
کراکینگ
اولفین‌های سبک

* عهده‌دار مکاتبات؛
رایانامه: ramin@modares.ac.ir
تلفن: ۸۲۸۸۳۳۱۵ ۲۱ ۹۸+
دورنگار: ۸۸۰۰۶۵۴۴ ۲۱ ۹۸+

چکیده

آنالیز ترمودینامیکی کراکینگ هگزان به کمک روش حداقل سازی انرژی آزاد گیبس و آنالیز واکنش‌های کلی به کمک قانون دوم ترمودینامیک صورت گرفته است. محصولات جانبی به سه دسته متان، آلکین‌ها و آروماتیک‌ها تقسیم بندی شده و مسیر محتمل برای تولید آنها بررسی شده است. اثر شرایط عملیاتی از قبیل دما و نسبت بخار به هگزان روی عملکرد کراکینگ مورد بررسی قرار گرفته است. نتایج نشان داد که میزان تبدیل هگزان با افزایش دما و محتوای بخارآب، افزایش می‌یابد. با افزایش دما، بازده تعادلی اولفین ابتدا افزایش یافته و در ادامه کاهش می‌یابد. در حضور متان، حداکثر مقدار بازده اولفین، افت نموده و به سمت دماهای پایین جابجا می‌شود. زمانیکه آروماتیک‌ها در لیست محصولات در نظر گرفته شد، بازده تولید اولفین‌ها ناچیز شد. تعادلات ترمودینامیکی پیش بینی می‌کند که با افزودن بخار آب به خوراک، به دلیل جلوگیری از واکنش‌های تشکیل آروماتیک‌ها، میزان تولید کک کاهش می‌یابد.